Article

Optical Gain of a Spherical InAs Quantum Dot under the Effects of the Intense Laser and Magnetic Fields

Noreddine Aghoutane [1], Laura M. Pérez [2,*], David Laroze [1], Pablo Díaz [3], Miguel Rivas [2], Mohamed El-Yadri [4], El Mustapha Feddi [4,5]

1 Instituto de Alta Investigación, CEDENNA, Universidad de Tarapacá, Casilla 7D, Arica 1000000, Chile; noreddine.aghoutane@gmail.com (N.A.); dlarozen@uta.cl (D.L.)
2 Departamento de Física, FACI, Universidad de Tarapacá, Casilla 7D, Arica 1000000, Chile; mrivas@uta.cl
3 Departamento de Ciencias Físicas, Universidad de La Frontera, Casilla 54-D, Temuco 4780000, Chile; pablo.diaz@ufrontera.cl
4 Group of Optoelectronic of Semiconductors and Nanomaterials, ENSAM, Mohammed V University, Rabat 10100, Morocco; m.elyadri@um5r.ac.ma (M.E.-Y.); e.feddi@um5r.ac.ma (E.M.F.)
5 Institute of Applied Physics, Mohammed VI Polytechnic University, Ben Guerir 43150, Morocco
* Correspondence: lperez@academicos.uta.cl

Abstract: In quantum dots, where confinement is strong, interactions between charge carriers play an essential role in the performance of semiconductor materials for optical gain. Therefore, understanding this phenomenon is critical for achieving new devices with enhanced features. In this context, the current study examines the optical properties of an exciton confined in a spherical InAs quantum dot under the influence of magnetic and intense laser fields. We investigate the oscillator strength, exciton lifetime, and optical gain, considering the effects of both external fields. We also pay particular attention to the influence of quantum dot size on the results. Our calculations show that the two external fields have opposite effects on our findings. Specifically, the applied magnetic field increases the oscillator strength while the intense laser reduces it. In addition, the optical gain peaks are redshifted under the application of the intense laser, whereas the magnetic field causes a blueshift of the peak threshold. We also find that both external perturbations significantly influence the exciton lifetime. Our study considers the outcomes of both the exciton's ground ($1s$) and first excited ($1p$) states. The theoretical results obtained in this study have promising implications for optoelectronic devices in the ∼3–4 μm wavelength range only through the control of quantum dot sizes and external perturbations.

Keywords: optical gain; exciton; lifetime; oscillator strength; quantum dot

1. Introduction

Nanoscale semiconductors (SCs) have been the subject of extensive study over the past two decades due to their intriguing optical properties that can be tailored based on their sizes and shapes. These properties can be harnessed for numerous applications, including lasers, solar cells, and light-emitting diodes, among others [1–7]. In these nanomaterials, charge carriers such as electrons and holes can combine through Coulomb interaction to form a correlated electron–hole pair known as an exciton distinguished by a lifetime. The lifetime of this exciton, along with the optical gain, is a crucial parameter in characterizing quantum dots (QDs). In low-dimension structures, the strong confinement of the charge carriers leads to the quantification of the energy levels in such a way that both the absorption and emission spectrums, arising from the transition between the discrete electron and hole energy levels, are highly sensitive to QD shapes and sizes [8,9]. In the literature, the optical properties of excitons, such as lifetime, optical gain (OG), and oscillator strengths (OS), have been extensively studied for different types of QDs [10–21]. For example, S. Yilmaz et al. [22] investigated the oscillator strengths for the intersubband transitions of

the impurity in a CdS–SiO$_2$ QD. Another study treated the OS of the exciton in big QD; the authors demonstrated that the Coulomb effect leads to very large oscillator strengths [23]. Y. Liu et al. investigated the optical gain of cubic and spherical CdSe QD; their findings show that the spherical dots have a higher optical amplification, while cubic dots have a wider gain spectrum [24]. Another work on the optical gain of a cubic CsPbBr$_3$ QD was carried out by J. Chen et al. [25] found that the peak of OG has a blueshift as the size of QD decreases. Q. Li et al. showed that the OG thresholds increase with the optical density at the excitation wavelength [26].

Furthermore, the effects of the external fields on the optical properties of QDs with different shapes and sizes have been reported in several studies [27–36]. J. Wang et al. investigated the effect of temperature on the exciton lifetime of PbS colloidal QDs [37]. S. K. Patra et al. conducted a theoretical and experimental analysis of the lifetimes in nonpolar InGaN/GaN QD; their findings show that the measured dots produce lifetime values of 250–300 ps [38]. B. Alén et al. carried out studies on the oscillator strengths and lifetime under the external electric field effect in self-assembled QD and rings; they demonstrated that the moderate electric field increases the lifetime of the exciton [39]. D. Makhlouf et al. studied the effects of applied electric and magnetic fields, pressure, and temperature on a lifetime in InAs/GaAs core/shell QD, and their results exhibit that the applied electric and magnetic fields have a significant impact on the carrier's lifetime [40]. The intense laser field effects on the exciton lifetime in GaAs–Ga$_{1-x}$Al$_x$As quantum wells show that the lifetime increases when the laser intensity increases [41]. Regarding optical gain, E. Owji et al. analyzed the effects of pressure, temperature, and size on the OG of spherical GaAs QDs in the presence of impurities; their results showed that increasing temperature produces a redshift of the OG, while applied pressure and increasing QD size show a blueshift of the peaks [42]. N. Saravanamoorthy et al. examined the magnetic field effect on the optical gain in a PbSe/CdSe core/shell QD; their calculations showed that the OG peak blueshifted with increasing the magnetic field [43].

As is known, external perturbations, such as the application of intense lasers and magnetic fields, can provide much valuable information about the optical properties of excitons confined in a QD. This information is important for fundamental physics and for new device applications. To our knowledge, the combined effects of these two types of fields on the oscillatory strength, lifetime, and optical gain have not been introduced theoretically for an exciton in a QD. Therefore, this study aims to improve our understanding of the effects of an intense laser and magnetic field on the optical properties of an exciton trapped in a quantum dot, which we have considered spherical and made of InAs. In addition, we have included the dependence of these optical properties on the size of the quantum dots in our analysis. The optical gain calculations are based on the density-matrix theory approach. The energies are determined using the effective mass approximation and a variational method with well-chosen wave functions for the ground (1s) and first excited (1p) states, taking into account the correlation between the electron and hole and the impact of laser intensity and magnetic field. The organization of this paper is as follows: the discussion of the theoretical background is presented in Section 2. Section 3 presents the numerical results and their interpretation. Finally, in Section 4, our conclusions are reported.

2. Background Theory

In this study, we investigate the behavior of an exciton confined in a spherical InAs quantum dot (QD), with radius R, under the influence of magnetic (B) and intense laser fields (ILF). The Hamiltonian that governs the electron–hole system (exciton) in the presence of both external fields can be expressed as:

$$H_X = \frac{1}{2\,m_e^*}\left(\vec{p_e} + \frac{e}{c}\vec{A_e}\right)^2 + \frac{1}{2\,m_h^*}\left(\vec{p_h} - \frac{e}{c}\vec{A_h}\right)^2 + V_c(\vec{\alpha}) + V_w^i \tag{1}$$

where $\overrightarrow{p_i} = -i\hbar\overrightarrow{\nabla}_i$ represents the momentum operator $(i = e, h)$, $\overrightarrow{A_i} = 1/2\,\overrightarrow{B} \wedge \overrightarrow{r_i}$ is the vector potential. m_e^* and m_h^* are the effective masses of electron and hole, respectively. $V_w^i = V_w^e + V_w^h$ is the electron and hole potential, given as follows:

$$V_w^i = \begin{cases} 0 & r_i < R \\ \infty & r_i > R \end{cases} \quad i = (e, h) \tag{2}$$

The choice of an infinite potential well can be justified with the very large band offsets between the InAs QD and the external medium, such as curable resin or another polymer with a very large gap. This results in a high probability of charge carriers being confined to the InAs QD, making the influence of the surrounding medium negligible.

$V_c(\overrightarrow{\alpha})$ is the dressed Coulomb interaction, which can be written as [44,45]:

$$V_c(\overrightarrow{\alpha}) = \frac{-e^2}{2\,\varepsilon_0}\left(\frac{1}{|\overrightarrow{r_e} - \overrightarrow{r_h} + \overrightarrow{\alpha}|} + \frac{1}{|\overrightarrow{r_e} - \overrightarrow{r_h} - \overrightarrow{\alpha}|}\right) \tag{3}$$

where $\alpha = eF/\mu\Omega^2 = (8\pi e^2 I/\mu^2 c^2 \Omega^4)^{1/2}$ is the laser-dressing parameter; F is the laser amplitude and Ω is the angular frequency; I (kW/cm^2) is the average intensity of the laser and $\mu = (\frac{1}{m_e^*} + \frac{1}{m_h^*})^{-1}$ is the exciton reduced mass; $\overrightarrow{r_e}$ and $\overrightarrow{r_h}$ are the electron and hole positions respectively.

The development of the Equation (1) leads to:

$$H_X = \frac{p_e^2}{2\,m_e^*} + \frac{p_h^2}{2\,m_h^*} + \frac{e^2}{2\,m_e^*c}A_e^2 + \frac{e^2}{2\,m_h^*c}A_h^2 + \frac{e}{m_e^*c}\overrightarrow{p_e}.\overrightarrow{A_e} - \frac{e}{m_h^*c}\overrightarrow{p_h}.\overrightarrow{A_h} + V_c(\overrightarrow{\alpha}) + V_w^i \tag{4}$$

with $\frac{e}{m_e^*c}\overrightarrow{p_e}.\overrightarrow{A_e} - \frac{e}{m_h^*c}\overrightarrow{p_h}.\overrightarrow{A_h} = \frac{eB\hbar}{2\,m_e^*c}L_{z_e} - \frac{eB\hbar}{2\,m_h^*c}L_{z_h}$ (L_{z_e} and L_{z_h} correspond respectively to the z-components of the angular momentum of the electron and hole). In fact, L_{z_e} and L_{z_h} do not give rise to any contribution because the corresponding states are invariant under rotation around the z-axis. Therefore, the magnetic operator M_n is reduced to:

$$M_n = \frac{e^2}{2\,m_e^*c}A_e^2 + \frac{e^2}{2\,m_h^*c}A_h^2. \tag{5}$$

By using the excitonic units $a_X = \hbar^2\varepsilon_0/e^2\mu$ for length and $R_X^* = \hbar^2/2\mu a_X^2$ as energy ($\sigma = m_e^*/m_h^*$ is the mass ratio), the Hamiltonian (4) becomes:

$$H_X = -\frac{1}{(1+\sigma)}\Delta_e - \frac{\sigma}{(1+\sigma)}\Delta_h - \tag{6}$$
$$\left(\frac{1}{|\overrightarrow{r_e} - \overrightarrow{r_h} + \overrightarrow{\alpha}|} + \frac{1}{|\overrightarrow{r_e} - \overrightarrow{r_h} - \overrightarrow{\alpha}|}\right) + M_n + V_w^i$$

By introducing the usual dimensionless parameter $\gamma = \hbar\omega_c/2R_X^*$ (ω_c is the effective cyclotron frequency), the magnetic operator M_n can be simplified as:

$$M_n = \frac{\gamma^2}{4(1+\sigma)}\left(r_e^2 - z_e^2 + \sigma(r_h^2 - z_h^2)\right) \tag{7}$$

The Hylleraas coordinates $(r_e, r_h, r_{eh}, z_e, z_h)$ are well-suited to describe a system with two bodies, and hence the Laplacian is given as $(i, j = e, h)$:

$$\Delta_i = \frac{\partial^2}{\partial r_i^2} + \frac{\partial^2}{\partial r_{eh}^2} + \left(\frac{r_i^2 - r_j^2 + r_{eh}^2}{r_i r_{eh}}\right)\frac{\partial^2}{\partial r_i \partial r_{eh}} + \frac{2}{r_i}\frac{\partial}{\partial r_i} + \frac{2}{r_{eh}}\frac{\partial}{\partial r_{eh}} + \frac{2z_i}{r_i} \tag{8}$$
$$\frac{\partial^2}{\partial z_i \partial r_i} + 2\left(\frac{z_i - z_j}{r_{eh}}\right)\frac{\partial^2}{\partial z_i \partial r_{eh}} + \frac{\partial^2}{\partial z_i^2}$$

The energies E_X^i and the corresponding wave functions Ψ_X^i of the exciton for the ground and the first excited states are solutions of the Schrödinger equation:

$$H_X \Psi_X^i = E_X^i \Psi_X^i \quad i = 1s,\ 1p \tag{9}$$

This equation can not be solved analytically, so the eigenvalues must be determined numerically using, in our case, a variational method. The trial wave function of the ground $1s$ ($n = 1, l = 0, m = 0$) and the first excited $1p$ ($n = 1, l = 1, m = 0$) states are constructed as multiplication of two functions of the electron and hole without Coulomb interaction, with three other functions describing the electron–hole interaction (exciton) and the distortion caused by the intense laser and magnetic fields. These wavefunctions can be written as:

$$\Psi_X^{1s} = N_0 J_0(r_e) Y_0^0(\theta_e, \varphi_e) J_0(r_h) Y_0^0(\theta_h, \varphi_h) e^{-\beta_{1s} r_{eh}} e^{\eta_{1s}\gamma^2(r_e^2 - z_e^2 + r_h^2 - z_h^2)} e^{\lambda_{1s}(z_e - z_h)} \tag{10}$$

$$\Psi_X^{1p} = N_1 J_1(r_e) Y_1^0(\theta_e, \varphi_e) J_1(r_h) Y_1^0(\theta_h, \varphi_h) e^{-\beta_{1p} r_{eh}} e^{\eta_{1p}\gamma^2(r_e^2 - z_e^2 + r_h^2 - z_h^2)} e^{\lambda_{1p}(z_e - z_h)} \tag{11}$$

J_0 and J_1 are the zero and first-order spherical Bessel functions respectively. $e^{-\beta_i r_{eh}}$ represents the Coulomb correlations between the charge carriers. $e^{\eta_i \gamma^2(r_e^2 - z_e^2 + r_h^2 - z_h^2)}$ and $e^{\lambda_i(z_e - z_h)}$ describe the effect of the magnetic and laser fields on the electron and hole, respectively ($i = 1s, 1p$). β_i, η_i and λ_i are the nonlinear variational parameters that must be determined to minimize the energies' mean values E_X^i:

$$E_X^i = \min_{\beta_i, \eta_i, \lambda_i} \frac{\langle \Psi_X^i | H_X | \Psi_X^i \rangle}{\langle \Psi_X^i | \Psi_X^i \rangle} \tag{12}$$

To gain insight into the optical properties of excitons confined in quantum dots, we first determine the oscillator strength associated with the recombination of the electron and hole pair. This oscillator strength is defined according to the equation [39,46]:

$$f_{osc} = \frac{E_p}{2 E_X^{t_i}} \left| \int \Psi_{eh}(r_e, r_h, z_e, z_h) \delta(\overrightarrow{r_e} - \overrightarrow{r_h}) dV \right|^2 \tag{13}$$

where E_p is Kane's energy and $E_X^{t_i}$ ($i = 1s, 1p$) is the exciton transition energy of the ground ($1s$), and the first excited ($1p$) states that must be determined by solving the Schrödinger equation.

By using the definition of the oscillator strength, the lifetime exciton of the $1s$ and $1p$ states can be calculated by the following expression [39,47]:

$$\tau = \frac{6\pi\varepsilon_0 m_0 c^3 \hbar^2}{e^2 n_r f_{osc}(E_X^{t_i})^2} \tag{14}$$

where c, n_r, m_0 and ε_0 are the speed of light, the refractive index of the studied material, the free electron mass, and the dielectric constant of the vacuum respectively.

Based on the density-matrix theory approach, the linear optical gain of QD is given as [48,49]:

$$G(E) = \frac{2\pi\hbar e^2 D_N}{n_r c \varepsilon_0 m_0^2} \sum_{c,v} \frac{|P_{cv}|^2 (f_c - f_v)}{E_X^{t_i}} B_{cv}(E - E_X^{t_i}) \tag{15}$$

f_c and f_v are the Fermi distribution function for the separate state of conduction and valence band, respectively; E represents the incident photon energy, D_N is the charge carriers density, and B_{cv} represents the broadening in the gain spectra for the QD which can be obtained by [50]:

$$B_{cv}(E - E_X^{t_i}) = \frac{\hbar\Gamma_{cv}/\pi}{(E - E_X^{t_i}) + (\hbar\Gamma_{cv})^2} \tag{16}$$

$\hbar\Gamma_{cv}$ is the homogeneous broadening due to the inter-band scattering, and P_{cv} represents the matrix element of the transition given by the relation:

$$|P_{cv}|^2 = M^2 I_{cv}^2 \tag{17}$$

I_{cv} describes the overlapping integral between the electron wavefunctions and the hole. M denotes the dipole moment element given as follows:

$$M^2 = \left(\frac{m_0}{m_e^*} - 1\right)\frac{E_g(E_g + \Delta)m_0}{6(E_g + 2\Delta/3)} \tag{18}$$

Δ is the spin-orbit interaction energy in the considered QD, and E_g denotes the band gap energy. The Fermi distribution function in the conduction and valence band is given by [51]:

$$f_{c(v)} = \frac{1}{1 + exp\left[(E_{n_{c(v)}} - E_{f_{c(v)}})/k_B T\right]} \tag{19}$$

where k_B is constant of Boltzmann and T represents the temperature; $E_{n_{c(v)}}$ and $E_{f_{c(v)}}$ are the energy state of the electron (hole) and the energy of quasi-Fermi states in the conduction (valence) band, respectively.

3. Results and Discussions

As mentioned above, the main objective of this work is to investigate the optical properties of a spherical InAs quantum dot (QD) in the presence of magnetic (B) and intense laser (ILF) fields. Table 1 lists the requisite parameters used in our calculations.

Table 1. Physical parameters of the studied materials [52,53].

m_e^*/m_0	m_h^*/m_0	ε_0	$E_g(eV)$	$E_P(eV)$	$\Delta(eV)$
0.023	0.41	15.15	0.418	21.5	0.38

The oscillator strength, which describes the efficiency of the light-matter interaction, is a key parameter controlling the optical properties of excitons and excitonic complexes in semiconductors. For this reason, we present in Figure 1 the evolution of the oscillator strength (f_{osc}) as a function of the QD radius for the excitonic ground state (1s) and first excited state (1p), and for various values of B and laser parameter α. As a first remark, the curves of f_{osc} augment monotonically with the QD radius R for both states, and the f_{osc} corresponding to the 1p state is higher than that of the 1s state, whatever the values of B and ILF; this result is attributed to the fact that the area occupied by the excitonic wave function becomes large when the QD radius increases, and therefore f_{osc} augments. When the magnetic field is applied for the small sizes (R < 18 nm), the oscillator strength is very slightly affected by this external perturbation and seems negligible. From R_0 = 18 nm, the effect of B on f_{osc} becomes more pronounced and augments as the QD radius increase. This behavior can be explained by the reinforcement of the overlapping wave function of the electron–hole pair (Equations (10) and (11)) caused by the applying magnetic field. The application of the laser (Figure 1b,c) shows a reduction in the f_{osc} values, which is more pronounced for larger QD sizes. This variation is related to the geometric modifications of the system caused by the ILF that affect the localization of the 1s and 1p exciton wave function inside the InAs QD. In summary, the oscillator strength evolution strongly depends on the QD sizes, magnetic field, and intense laser, and the variations in these parameters lead to changes in the exciton's wave function and transition energies, and thus in f_{osc}.

Next, we examine the evolution of the exciton lifetime, which depends mainly on the changes in the excitonic transition energy and the oscillator strength (as per Equation (14)). Figure 2a,b indicate the variation of the exciton lifetime (τ) as a function of the QD radius for the 1p and 1s states, respectively. The graphs indicate that the exciton lifetime increases

with the increase of the QD radius, and in the case of a strong confinement regime, the lifetime is very short, about 300 ps for the 1*s* state and around 270 ps for the 1*p* state. Our obtained values are inferior to those found for the lens-shaped InAs/GaAs and InAs/InP QDs, where τ is approximately 1 ns and 2 ns, respectively [54]. This difference is attributed to the shape of the QD and the exterior medium. We assume that the InAs QD is immersed in a matrix with a very large band offset (infinite confinement). For the large QD sizes, we find that the exciton lifetime related to the 1*s* state becomes very large, while for the 1*p* state, the τ increase remains small. These variations are due to the wave function expansion that describes electron–hole interaction and the reduction of the excitonic energy when the QD size increases. Note that the formula for the exciton lifetime is inversely proportional to the transition energy and the oscillator strength (Equation (14)). The variations of these two parameters are more significant for the 1*s* state than for the 1*p* state, leading to a more pronounced evolution of the 1*s* exciton lifetime than that obtained for the first excited state 1*p*.
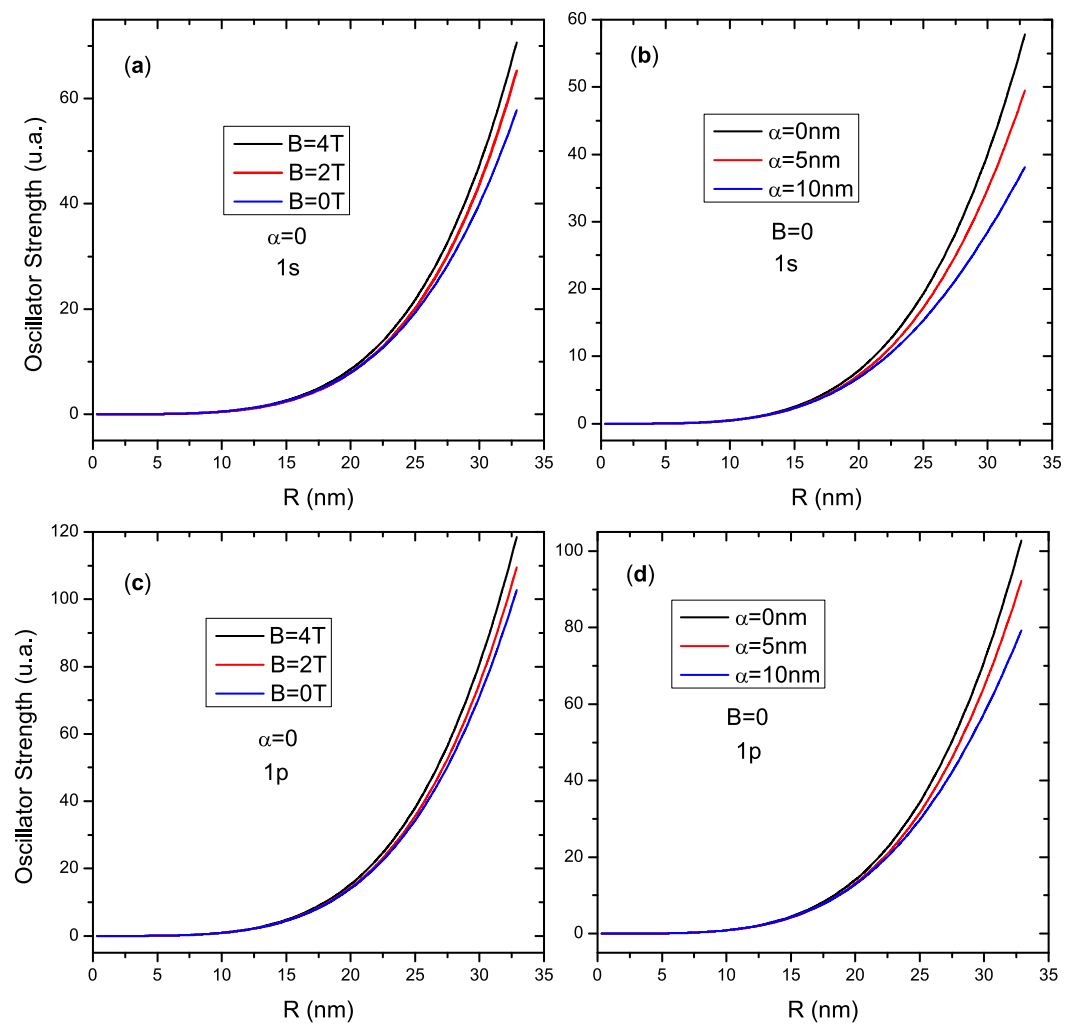

Figure 1. Variation of the exciton oscillator strength as a function of the QD radius (R) for: (**a**) 1*s* state, for B = 0, 2, and 4 T, and for α = 0 nm. (**b**) 1*s* state, for α = 0, 5 and 10 nm, and for B = 0 T. (**c**) 1*p* state, for B = 0, 2 and 4 T, and for α = 0 nm. (**d**) 1*p* state, for α = 0, 5 and 10 nm, and for B = 0 T.

In Figure 3a,b, we present the variation of the exciton lifetime as a function of the magnetic field intensities for the 1*s* and 1*p* states, for R = 6 nm and R = 12 nm respectively. The results for R = 6 nm, presented in Figure 3a, show that the exciton lifetime is a decreasing function with the applying magnetic field due to the augmentation of the f_{ocs} and the excitonic transition energy influenced by this applied field. It is also noteworthy

that the effect of B on τ is less significant for the low B intensities. We can also observe that the magnetic field impact on the exciton lifetime is more important for the 1s state (black line) than for the 1p state (blue line). The results for R = 12 nm, presented in Figure 3b, show the same behavior as that obtained for R = 6 nm, but with a larger range for τ values. This difference is attributed to the confinement effect.
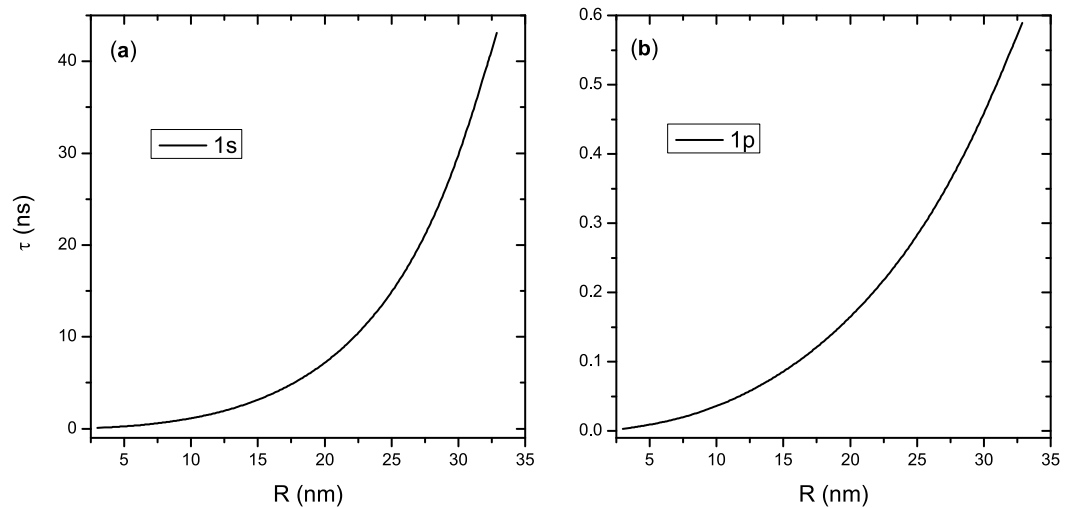

Figure 2. Evolution of the exciton lifetime (τ) as a function of the QD radius (R) for: (**a**) ground state 1s. (**b**) first excited state 1p.

In the following, we analyze the effect of the intense laser field on the exciton lifetime. Figure 4a,b illustrate the evolution of τ as a function of the laser parameter α for 1s and 1p states, for R = 6 nm and R = 12 nm respectively. The results for R = 6 nm show that the exciton lifetime reduces when the α parameter increases before reaching a minimum at $\alpha \simeq 10$ nm and $\alpha \simeq 8$ nm for the 1s states (black line) and 1p states (blue line), respectively, and then increases. This behavior is attributed to modifying the system geometry under the effect of this external parameter, which affects the transition energy, the dipole matrix element, and oscillator strength related to the excitonic wavefunction of the 1s and 1p states. The results for R = 12 nm, presented in Figure 4b, show that the τ variations follow the same evolution found for R = 6 nm, but for this case, the minimum of the curve related to the lifetime moves to the higher values of α ($\simeq 11$ nm). We also note that the exciton lifetime is more affected when the laser intensities become large ($\alpha > 18$).
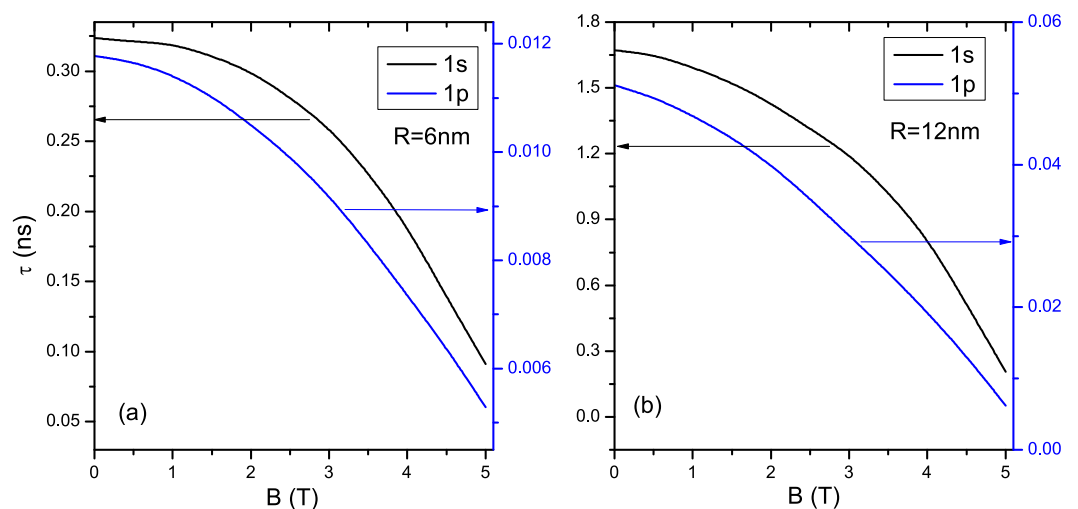

Figure 3. Variations of the exciton lifetime (τ) as a function of the magnetic field values for both 1s and 1p states with (**a**) R = 6 nm and (**b**) R = 12 nm.
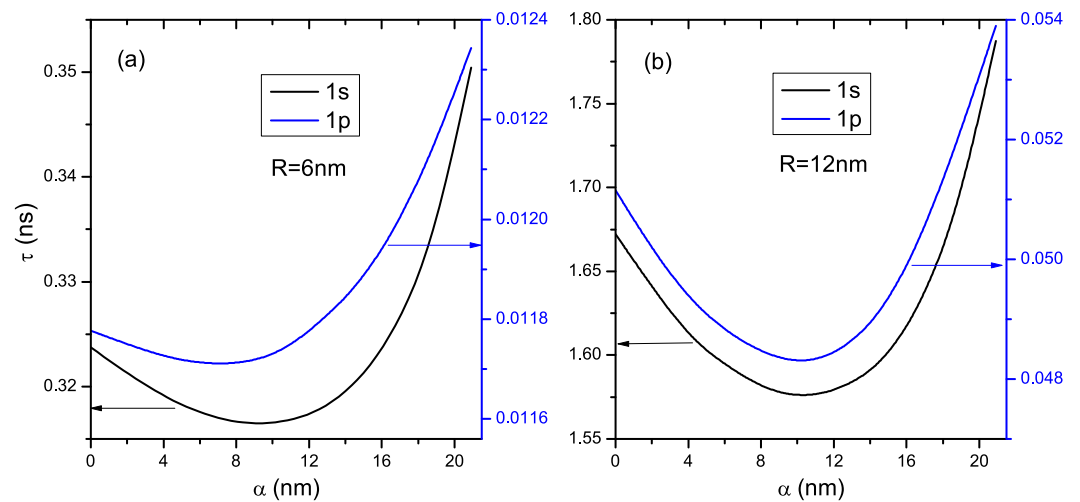
Figure 4. Variations of the exciton lifetime (τ) as a function of the laser parameter (α) for both 1*s* and 1*p* states with (**a**) R = 6 nm and (**b**) R = 12 nm.

To explore further, we analyzed the impact of quantum dot size, magnetic field, and intense laser field on optical gain. Our calculations were performed at room temperature (T = 300 K), and the charge carrier density was taken as 2×10^{24} m^{-3}. Figure 5a shows the variations of the optical gain as a function of photon energy for R = 6 nm and R = 12 nm, and for the states 1*s* and 1*p*, in the absence of the external fields. Referring to Equation (15), the linear optical gain depends on the band gap, transition matrix elements, and Fermi factors. The excitonic energy transitions dictate the peak position of the gain spectrum. It is noteworthy that, by increasing the QD radii (for both states), the optical gain spectrum shifts towards the lower energy regions (redshift), and the peak intensity is also reduced due to the confinement effect. It is known that the energy of the electron and hole decreases when the QD radius increases because of the propagation of the electronic density inside the dot, i.e., the Coulomb interaction becomes weak, and thus the system relaxes. The transition energies become less important, leading to the observed redshift when the QD radius increases. Additionally, we observe that, for a given QD radius, the threshold for the observation of optical gain of the 1*s* state is found in the region of the lower energies compared to that of the 1*p* state with a reduction in the peak intensities. Figure 5b illustrates the effect of magnetic and intense laser fields on the excitonic optical gain of the 1*s* state for a quantum dot with radius R = 6 nm. The OG variation is show for these case: (B = 0, $\alpha = 0$), (B = 4 T, $\alpha = 0$), and ($\alpha = 10$ nm, B = 0). It can be observed that increasing the magnetic field causes the OG peak to shift to higher energy regions (blue shifted), with an increase in intensity. Conversely, the intense laser field leads to a peak redshift with a reduction in the intensity due to the reduced transition energies and the wavefunctions of the electron and hole. In Figure 5c, the evolution of the optical gain of the 1*p* state under the same conditions is plotted. The curves show similar behaviors to those obtained for the 1*s* state but with changes in the absorption threshold values due to differences in the parameters between the two states.

Finally, it should be noted that the absorbed photon thresholds were found to be approximately 2.99 μm and 3.1 μm, for R = 6 nm, and 3.74 μm and 3.99 μm for R = 12 nm, for the 1*s* and 1*p* states respectively. These wavelength ranges have potential applications in various fields, such as developing highly efficient laser diodes and thermo-photovoltaic converters, which convert heat directly into electrical power. By controlling the size of the quantum dots and the external fields applied, it may be possible to tune further the absorbed photon thresholds and optimize the performance of these devices. Additionally, these findings may have implications for other research areas, such as designing new materials for optoelectronics and photonics.
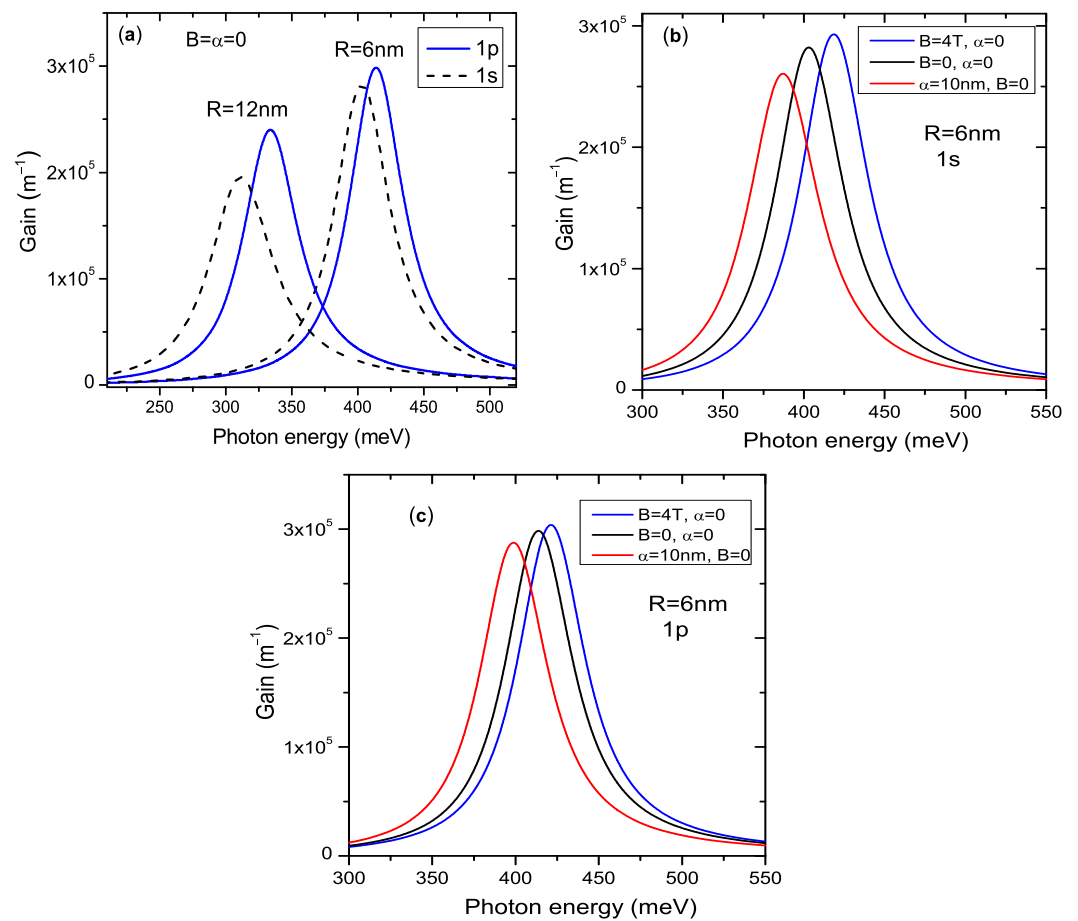
Figure 5. The optical gain variation versus the photon energy for (**a**) 1*s* and 1*p* states, for R = 6 nm and $R = 12$ nm, without magnetic and laser fields effect. (**b,c**) corresponding to the 1*s* and 1*p* states, respectively, for (B = 0, α = 0), (B = 4 T, α = 0), and (α = 10 nm, B = 0), with R = 6 nm.

4. Conclusions

In summary, we have theoretically studied the effects of the sizes, magnetic, and intense laser fields on the optical properties of an exciton trapped on an InAs quantum dot. We have shown that the exciton lifetime and oscillator strength are increasing function with the QD sizes. They are strongly affected by the application of both external fields. Our results also show that the optical gain threshold is redshifted when the laser intensity and QD size increase. The applied magnetic field causes a blue shift of the peak threshold (the two fields have an antagonistic effect). Our study is consecrated to the ground and first excited states of the exciton, where we find that the threshold of optical gain of the ground state is located in the region of the lower energies compared to that of the first excited state. Our findings can provide more comprehension of the physics behind the optical properties of an exciton trapped on a spherical QD and inspire more applications in novel optoelectronic devices for a ∼3–4 μm wavelength range and that, by controlling the sizes and external perturbations.

Author Contributions: Conceptualization, N.A. and E.M.F.; methodology, N.A. and L.M.P.; software, N.A. and D.L.; formal analysis, N.A., M.R., M.E.-Y. and E.M.F.; investigation, N.A., P.D. and M.E.-Y.; resources, L.M.P. and D.L.; data curation, N.A. and L.M.P.; writing—original draft preparation, N.A., E.M.F. and L.M.P.; writing—review and editing, N.A., M.E.-Y. and D.L.; visualization, L.M.P., M.R., P.D. and M.E.-Y.; supervision, D.L. and E.M.F.; project administration, N.A., D.L. and E.M.F. All authors have read and agreed to the published version of the manuscript.

Data Availability Statement: The data that support the findings of this study are available on reasonable request from the corresponding author.

Conflicts of Interest: All authors declare no conflict of interest.

References

1. Tong, C.; Jagadish, C. *Nanoscale Semiconductor Lasers*, 1st ed.; Elsevier Science: Amsterdam, The Netherlands, 2019.
2. Verma, V. B.; Elarde, V. C. Nanoscale selective area epitaxy: From semiconductor lasers to single-photon sources. *Prog. Quantum. Electron.* **2021**, *75*, 100305. [CrossRef]
3. Zhou, C.; Pina, J.M.; Zhu, T.; Parmar, D.H.; Chang, H.; Yu, J.; Yuan, F.; Bappi, G.; Hou, Y.; Zheng, X.; et al. Quantum dot self-assembly enables low-threshold lasing. *Adv. Sci.* **2021**, *8*, 2101125. [CrossRef] [PubMed]
4. Lee, S.; Lee, J.S.; Jang, J.; Hong, K.-H.; Lee, D.-K.; Song, S.; Kim, K.; Eo, Y.-J.; Yun, J.H.; Gwak, J.; et al. Robust nanoscale contact of silver nanowire electrodes to semiconductors to achieve high performance chalcogenide thin film solar cells. *Nano Energy* **2018**, *53*, 675–682. [CrossRef]
5. Swarnkar, A.; Marshall, A.R.; Sanehira, E.M.; Chernomordik, B.D.; Moore, D.T.; Christians, J.A.; Chakrabarti, T.; Luther, J.M. Quantum dot–induced phase stabilization of $\alpha - CsPbI_3$ perovskite for high-efficiency photovoltaics. *Science* **2016**, *354*, 92–96. [CrossRef] [PubMed]
6. Fox, M.; Ispasoiu, R. Quantum wells, superlattices, and band-gap engineering. In *Springer Handbook of Electronic and Photonic Materials*; Springer: Cham, Switzerland, 2017.
7. Wu, J.; Fang, G.; Zhang, Y.; Biswas, N.; Ji, N.; Xu, W.; Dong, B.; Liu, N. Semiconductor nanomaterial-based polarized light emission: From materials to light emitting diodes. *Sci. China Mater.* **2023**, *66*, 1257–1282. [CrossRef]
8. Kim, S.H.; Man, M.T.; Lee, J.W.; Park, K.D.; Lee, H.S. Influence of size and shape anisotropy on optical properties of CdSe quantum dots. *Nanomaterials* **2020**, *10*, 1589. [CrossRef]
9. Torres-Gomez, N.; Garcia-Gutierrez, D.F.; Lara-Canche, A.R.; Triana-Cruz, L.; Arizpe-Zapata, J.A.; Garcia-Gutierrez, D.I. Absorption and emission in the visible range by ultra-small PbS quantum dots in the strong quantum confinement regime with S-terminated surfaces capped with diphenylphosphine. *J. Alloys Compd.* **2021**, *860*, 158443. [CrossRef]
10. Heyn, C.; Strelow, C.; Hansen, W. Excitonic lifetimes in single GaAs quantum dots fabricated by local droplet etching. *New J. Phys.* **2012**, *14*, 053004. [CrossRef]
11. Geuchies, J.J.; Brynjarsson, B.; Grimaldi, G.; Gudjonsdottir, S.; van der Stam, W.; Evers, W.H.; Houtepen, A.J. Quantitative electrochemical control over optical gain in quantum-dot solids. *ACS Nano* **2021**, *15*, 377–386. [CrossRef]
12. Bisschop, S.; Geiregat, P.; Aubert, T.; Hens, Z. The impact of core/shell sizes on the optical gain characteristics of CdSe/CdS quantum dots. *ACS Nano* **2018**, *12*, 9011–9021. [CrossRef]
13. Wu, K.; Park, Y.S.; Lim, J.; Klimov, V.I. Towards zero-threshold optical gain using charged semiconductor quantum dots. *Nat. Nanotechnol.* **2017**, *12*, 1140–1147. [CrossRef] [PubMed]
14. Ji, Z.M.; Song, Z.G. Exciton radiative lifetime in CdSe quantum dots. *J. Semicond.* **2023**, *44*, 032702. [CrossRef]
15. Goupalov, V.; Ivchenko, E.L.; Nestoklon, M.O. Optical transitions, exciton radiative decay, and valley coherence in lead chalcogenide quantum dots. *Phys. Rev. B* **2022**, *106*, 125301. [CrossRef]
16. Naimi, Y. Comment on "Magnetic field effects on oscillator strength, dipole polarizability and refractive index changes in spherical quantum dot". *Phys. Lett.* **2021**, *767*, 138380. [CrossRef]
17. Makhlouf, D.; Choubani, M.; Saidi, F.; Maaref, H. Enhancement of transition lifetime, linear and nonlinear optical properties in laterally coupled lens-shaped quantum dots for Tera-Hertz range. *Physica E* **2018**, *103*, 87–92. [CrossRef]
18. Lim, J.; Park, Y.S.; Klimov, V.I. Optical gain in colloidal quantum dots achieved with direct-current electrical pumping. *Nat. Mater.* **2018**, *17*, 42–49. [CrossRef] [PubMed]
19. Jung, H.; Park, Y.S.; Ahn, N.; Lim, J.; Fedin, I.; Livache, C.; Klimov, V.I. Two-band optical gain and ultrabright electroluminescence from colloidal quantum dots at 1000 A cm^{-1}. *Nat. Commun.* **2022**, *13*, 3734. [CrossRef]
20. Taghipour, N.; Delikanli, S.; Shendre, S.; Sak, M.; Li, M.; Isik, F.; Tanriover, I.; Guzelturk, B.; Sum, T.C.; Demir, H.V. Sub-single exciton optical gain threshold in colloidal semiconductor quantum wells with gradient alloy shelling. *Nat. Commun.* **2020**, *11*, 3305. [CrossRef]
21. Yang, W.; Yang, Y.; Kaledin, A.L.; He, S.; Jin, T.; McBride, J.R.; Lian, T. Surface passivation extends single and biexciton lifetimes of InP quantum dots. *Chem. Sci.* **2020**, *11*, 5779–5789. [CrossRef]
22. Yilmaz, S.; Safak, H. Oscillator strengths for the intersubband transitions in a $CdS - SiO_2$ quantum dot with hydrogenic impurity. *Physica E* **2007**, *36*, 40–44. [CrossRef]
23. Stobbe, S.; Schlereth, T.W.; Höfling, S.; Forchel, A.; Hvam, J.M.; Lodahl, P. Large quantum dots with small oscillator strength. *Phys. Rev. B* **2010**, *82*, 233302. [CrossRef]
24. Liu, Y.; Bose, S.; Fan, W. Effect of size and shape on electronic and optical properties of CdSe quantum dots. *Optik* **2018**, *155*, 242–250. [CrossRef]
25. Chen, Q.; Song, Z.; Zhang, D.; Sun, H.; Fan, W. Effect of size on the electronic structure and optical properties of cubic $CsPbBr_3$ quantum dots. *IEEE J. Quantum Electron.* **2020**, *56*, 1–7. [CrossRef]

26.　Li, Q.; Lian, T. A model for optical gain in colloidal nanoplatelets. *Chem. Sci.* **2018**, *9*, 728–734. [CrossRef] [PubMed]

27.　Deng, Y.; Lin, X.; Fang, W.; Di, D.; Wang, L.; Friend, R.H.; Peng, X.; Jin, Y. Deciphering exciton-generation processes in quantum-dot electroluminescence. *Nat. Commun.* **2020**, *11*, 2309. [CrossRef] [PubMed]

28.　Wang, Z.; Sun, H.; Zhang, Q.; Feng, J.; Zhang, J.; Li, Y.; Ning, C.Z. Excitonic complexes and optical gain in two-dimensional molybdenum ditelluride well below the Mott transition. *Light Sci. Appl.* **2020**, *9*, 39. [CrossRef] [PubMed]

29.　Stachurski, J.; Tamariz, S.; Callsen, G.; Butté, R.; Grandjean, N. Single photon emission and recombination dynamics in self-assembled GaN/AlN quantum dots. *Light Sci. Appl.* **2022**, *11*, 114. [CrossRef]

30.　Bleyan, Y.Y.; Mantashyan, P.A.; Kazaryan, E.M.; Sarkisyan, H.A.; Accorsi, G.; Baskoutas, S.; Hayrapetyan, D.B. Non-linear optical properties of biexciton in ellipsoidal quantum dot. *Nanomaterials* **2022**, *12*, 1412. [CrossRef]

31.　Barjon, J. Luminescence spectroscopy of bound excitons in diamond. *Phys. Status Solidi A* **2017**, *214*, 1700402. [CrossRef]

32.　Große, J.; Mrowiński, P.; Srocka, N.; Reitzenstein, S. Quantum efficiency and oscillator strength of InGaAs quantum dots for single-photon sources emitting in the telecommunication O-band. *Appl. Phys. Lett.* **2021**, *119*, 061103. [CrossRef]

33.　Aghoutane, N.; El-Yadri, M.; El Aouami, A.; Feddi, E.; Dujardin, F.; El Haouari, M. Optical absorption of excitons in strained quasi 2D GaN quantum dot. *Phys. Status Solidi B* **2019**, *256*, 1800361. [CrossRef]

34.　Aghoutane, N.; Pérez, L.M.; Tiutiunnyk, A.; Laroze, D.; Baskoutas, S.; Dujardin, F.; El Fatimy, A.; El-Yadri, M.; Feddi, E. Adjustment of terahertz properties assigned to the first lowest transition of (D^+, X) excitonic complex in a single spherical quantum dot using temperature and pressure. *Appl. Sci.* **2021**, *11*, 5969. [CrossRef]

35.　Kumar, D.; Negi, C.M.S.; Kumar, J. Temperature effect on optical gain of CdSe/ZnSe quantum dots. In *Advances in Optical Science and Engineering*; Springer Proceedings in Physics; Springer: New Delhi, India, 2015; Volume 163, pp. 563–569.

36.　Geiregat, P.; Rodá, C.; Tanghe, I.; Singh, S.; Di Giacomo, A.; Lebrun, D.; Grimaldi, G.; Maes, J.; Van Thourhout, D.; Moreels, I.; et al. Localization-limited exciton oscillator strength in colloidal CdSe nanoplatelets revealed by the optically induced stark effect. *Light Sci. Appl.* **2021**, *10*, 5969. [CrossRef] [PubMed]

37.　Wang, J.; Mandelis, A.; Melnikov, A.; Hoogland, S.; Sargent, E.H. Exciton lifetime broadening and distribution profiles of PbS colloidal quantum dot thin films using frequency- and temperature-scanned photocarrier radiometry. *J. Phys. Chem. C* **2013**, *117*, 23333–23348. [CrossRef]

38.　Patra, S.K.; Wang, T.; Puchtler, T.J.; Zhu, T.; Oliver, R.A.; Taylor, R.A.; Schulz, S. Theoretical and experimental analysis of radiative recombination lifetimes in nonpolar InGaN/GaN quantum dots. *Phys. Status Solidi B* **2017**, *254*, 1600675. [CrossRef]

39.　Alén, B.; Bosch, J.; Granados, D.; Martínez-Pastor, J.; García, J.M.; González, L. Oscillator strength reduction induced by external electric fields in self-assembled quantum dots and rings. *Phys. Rev. B* **2007**, *75*, 045319. [CrossRef]

40.　Makhlouf, D.; Choubani, M.; Saidi, F.; Maaref, H. Applied electric and magnetic fields effects on the nonlinear optical rectification and the carrier's transition lifetime in InAs/GaAs core/shel quantum dot. *Mater. Chem. Phys.* **2021**, *267*, 124660. [CrossRef]

41.　Niculescu, E.C.; Eseanu, N.; Spandonide, A. Laser field effects on the interband transitions in differently shaped quantum wells. *UPB Sci. Bull. Ser. A* **2008**, *77*, 281–292.

42.　Owji, E.; Keshavarz, A.; Mokhtari, H. The effects of temperature, hydrostatic pressure and size on optical gain for GaAs spherical quantum dot laser with hydrogen impurity. *Superlattice Microst.* **2016**, *98*, 276–282. [CrossRef]

43.　Saravanamoorthy, S.N.; Peter, A.J.; Lee, C.W. Optical peak gain in a PbSe/CdSe core-shell quantum dot in the presence of magnetic field for mid-infrared laser applications. *Chem. Phys.* **2017**, *483-484*, 1–6. [CrossRef]

44.　Burileanu, L.M. Photoionization cross-section of donor impurity in spherical quantum dots under electric and intense laser fields. *J. Lumin.* **2014**, *145*, 684–689. [CrossRef]

45.　Ehlotzky, F. Positronium decay in intense high frequency laser fields. *Phys. Lett. A* **1988**, *126*, 524–527. [CrossRef]

46.　Davies, J.H. *The Physics of Low-Dimensional Semiconductors: An Introduction*; Cambridge University Press: London, UK, 1996.

47.　Alén, B.; Bickel, F.; Karrai, K.; Warburton, R.J.; Petroff, P.M. Stark-shift modulation absorption spectroscopy of single quantum dots. *Appl. Phys. Lett.* **2003**, *83*, 2235. [CrossRef]

48.　Chuang, S.L. Physics of photonic devices. In *Physics of Photonic Devices*; Wiley: Hoboken, NJ, USA, 2009; pp. 365–372.

49.　Sugawara, M.; Mukai, K.; Nakata, Y.; Ishikawa, H.; Sakamoto, A. Effect of homogeneous broadening of optical gain on lasing spectra in self-assembled In$_x$Ga$_{1-x}$As/GaAs quantum dot lasers. *Phys. Rev. B* **2000**, *61*, 7595–7603. [CrossRef]

50.　Sakamoto, A.; Sugawara, M. Theoretical calculation of lasing spectra of quantum-dot lasers: Effect of homogeneous broadening of optical gain. *IEEE Photonics Technol. Lett.* **2000**, *12*, 107–109. [CrossRef]

51.　Ashcroft, N.W.; Mermin, N.D. *Solid State Physics*; Saunders: Philadelphia, PA, USA, 1976.

52.　Stier, O.; Grundmann, M.; Bimberg, D. Electronic and optical properties of strained quantum dots modeled by 8-band k.p theory. *Phys. Rev. B* **1999**, *59*, 5688. [CrossRef]

53.　Warburton, R.J.; Gauer, C.; Wixforth, A.; Kotthaus, J.P. Intersubband resonances in InAs/AlSb quantum wells: Selection rules, matrix elements, and the depolarization field. *Phys. Rev. B* **1996**, *53*, 7903. [CrossRef]

54.　Gong, M.; Zhang, W.; Guo, G.C.; He, L. Atomistic pseudopotential theory of optical properties of exciton complexes in InAs/InP quantum dots. *Appl. Phys. Lett.* **2011**, *99*, 231106. [CrossRef]